Cell

Kynurenic Acid Is a Nutritional Cue that Enables Behavioral Plasticity

George A. Lemieux,[1] Katherine A. Cunningham,[1] Lin Lin,[1] Fahima Mayer,[1] Zena Werb,[2] and Kaveh Ashrafi[1,*]
[1]Department of Physiology, University of California, San Francisco, San Francisco, CA 94158-2240, USA
[2]Department of Anatomy, University of California, San Francisco, San Francisco, CA 94143-0452, USA
*Correspondence: kaveh.ashrafi@ucsf.edu
http://dx.doi.org/10.1016/j.cell.2014.12.028

SUMMARY

The kynurenine pathway of tryptophan metabolism is involved in the pathogenesis of several brain diseases, but its physiological functions remain unclear. We report that kynurenic acid, a metabolite in this pathway, functions as a regulator of food-dependent behavioral plasticity in *C. elegans*. The experience of fasting in *C. elegans* alters a variety of behaviors, including feeding rate, when food is encountered post-fast. Levels of neurally produced kynurenic acid are depleted by fasting, leading to activation of NMDA-receptor-expressing interneurons and initiation of a neuropeptide-y-like signaling axis that promotes elevated feeding through enhanced serotonin release when animals re-encounter food. Upon refeeding, kynurenic acid levels are eventually replenished, ending the elevated feeding period. Because tryptophan is an essential amino acid, these findings suggest that a physiological role of kynurenic acid is in directly linking metabolism to activity of NMDA and serotonergic circuits, which regulate a broad range of behaviors and physiologies.

INTRODUCTION

Imbalances in brain levels of metabolites derived from tryptophan degradation via the kynurenine pathway (KP) have been linked to a variety of neurodegenerative and psychiatric disorders (Schwarcz et al., 2012). Altered brain or cerebrospinal fluid levels of kynurenic acid (KynA) and/or quinolinic acid are associated with schizophrenia (Erhardt et al., 2001; Schwarcz et al., 2001), Alzheimer's, and Huntington's diseases (Beal et al., 1992; Heyes et al., 1992) and depression (Steiner et al., 2011; Erhardt et al., 2013). Genetic and pharmacological blockade of the KP ameliorates neurodegeneration and protein aggregation in diverse model organisms (Campesan et al., 2011; Zwilling et al., 2011; van der Goot et al., 2012), whereas the beneficial effects of exercise on symptoms of depression have been attributed to altered peripheral KP metabolism (Agudelo et al., 2014). Despite these associations, the physiological regulation of brain levels of KP metabolites and their normal physiological roles remain ill defined.

Several intermediates of the KP have distinct neuro- and immune-modulatory functions. For example, KynA inhibits and quinolinic acid activates glutamatergic neurotransmission (Perkins and Stone, 1982; Hilmas et al., 2001), leading to the suggestion that the associations of the KP with CNS disorders derive from modulation of glutamate excitotoxicity (Andiné et al., 1988; Carpenedo et al., 2001; Foster et al., 1984). Additionally, the serotonin-kynurenine hypothesis of depression advanced the idea that disregulated shunting of tryptophan through the KP negatively impacts serotonin levels (Lapin and Oxenkrug, 1969). However, direct physiological evidence of KP metabolic competition limiting serotonin biosynthesis has been lacking.

C. elegans display food-related behavioral plasticity (Sengupta, 2013; Douglas et al., 2005). For example, when *C. elegans* deplete their local food source, they reduce their food intake behavior and increase their locomotory rate to forage for food, behaviors that depend on changes in serotonin signaling (Avery and Horvitz, 1990; Sawin et al., 2000; Hills et al., 2004). Upon encountering a new food source, *C. elegans* resume their ad libitum feeding and movement rates. However, if *C. elegans* experience a period of fasting before encountering food, they temporarily increase their feeding rate and slow their movement beyond the levels seen in ad-libitum-fed animals once they are back on food (Avery and Horvitz, 1990; Sawin et al., 2000). These behaviors presumably allow food-deprived animals to consume more food and rapidly recover physiologic functions post-fast. How the experience of fasting further modulates responses to food is poorly understood.

Here, we show that KynA serves as an internal gauge of nutrient availability to modulate feeding behavior in *C. elegans*. Depletion of KynA during fasting from the nervous system is required for the hyperactivation of feeding in *C. elegans* when they re-encounter food. Feeding then leads to replenishment of the KynA, ending the hyperactive feeding state. KynA depletion is sensed by neurons that express NMDA-type ionotropic glutamate receptors (NMDA-r) whose activity is communicated to serotonergic sensory neurons via a neuropeptide signaling axis. Given that many of the regulatory modules discovered in the context of *C. elegans* feeding behavior are conserved in the mammalian brain, the role of KynA as a neurally produced gauge of the peripheral metabolic state that controls serotonin signaling is likely to be well conserved.

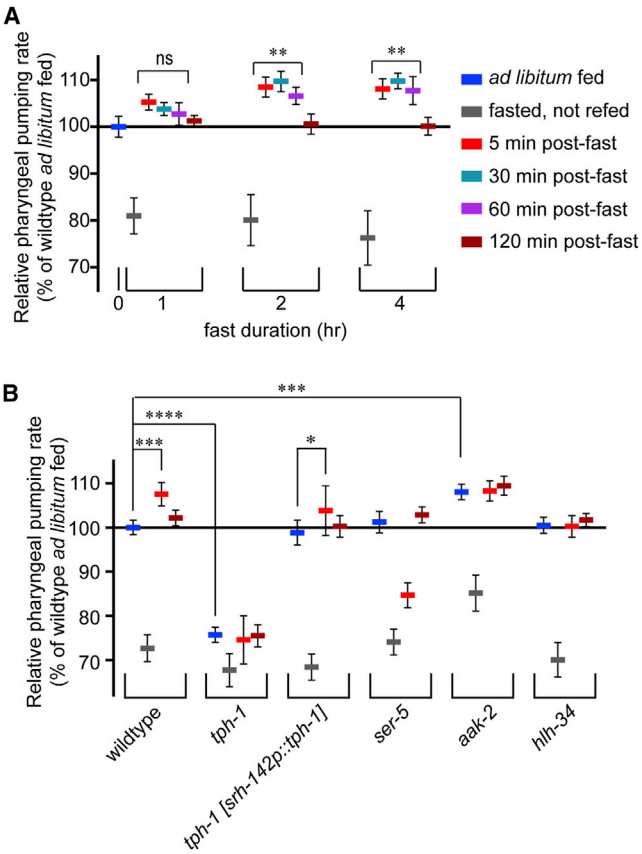

Figure 1. Post-Fast Hyperactive Feeding Requires Serotonin Signaling

(A) Animals were fasted for 1, 2, or 4 hr, and the pharyngeal pumping rate was measured before exposure to food and 5, 30, 60, and 120 min post-fast. To facilitate visualization of data pertaining to changes in pumping rate, all feeding data are presented with the x axis defining the ad-libitum-fed wild-type rate. n = 10–14 animals per condition; ns, $p > 0.05$ and $^{**}p < 0.01$ compared to ad-libitum-fed ANOVA (Dunnett).

(B) Pharyngeal pumping rates of wild-type, mutant, or transgenic animals at the indicated fasting and refeeding periods. n = 10 animals per condition. $^{*}p < 0.05$, $^{***}p < 0.001$, and $^{****}p < 0.0001$ ANOVA (Sidak). In (A) and (B), error bars indicate 95% confidence interval (c.i.).

See also Figure S1 and Table S1.

RESULTS

Fasting Induces a Serotonin-Regulated Hyperactive Feeding State upon Food Re-exposure

C. elegans actively ingest food through regular, coordinated muscular contractions of the pharynx that concentrate, disrupt, and pump bacterial food into their intestinal lumens (Avery and You, 2012). The pharyngeal pumping rate correlates with food intake (Avery and Horvitz, 1990; Avery and You, 2012). Except for periods of developmental arrest or larval molts, when cultured on *E. coli* OP50, *C. elegans* exhibit continuous pumping with brief intermittent pauses (Avery and You, 2012; You et al., 2008). *C. elegans* change their pumping rates relative to food availability and the experience of fasting by reducing the rates when fasted, and, as we will describe in detail below, they temporarily hyperactivate it relative to the ad-libitum-fed state when they are reintroduced to food post-fast (Avery and Horvitz, 1990).

To characterize the post-fast overfeeding behavior, we subjected *C. elegans* to 1, 2, or 4 hr of fasting and measured pumping rates immediately before and after returning to ad libitum access to food for 5, 30, 60, and 120 min (Figure 1A). Each of these fast intervals caused the same extent of reduction in pumping. In turn, all fasted animals resumed rapid pumping upon returning to food. However, upon introduction of food, animals that had fasted for more than 1 hr exhibited hyperactive feeding. This hyperactive feeding state was temporary, persisting for 1 hr before subsiding to ad libitum rates that were intermediate between the depressed fasting rates and the hyperactive rate seen post-fast (Figure 1A). The extent and duration of the overfeeding were not enhanced in animals that had been fasted for 4 hr versus those fasted for 2 hr (Figure 1A). Although in absolute terms the noted changes in pumping rate are small, representing the normal physiologic range of this behavior, the pharyngeal pumping rate is a robustly quantitative trait due to its small variance.

To understand how the post-fast hyperactive feeding state is regulated, we first examined serotonin signaling. Serotonin-deficient *tph-1* mutants exhibit reduced pharyngeal pumping relative to wild-type animals (Sze et al., 2000), and restoration of *tph-1* to only the ADF neurons, a pair of serotonergic head sensory neurons, confers wild-type pumping under ad-libitum-fed conditions (Cunningham et al., 2012) and upregulated pumping in response to familiar food (Song et al., 2013). We found that serotonin deficiency also abrogates fasting-induced hyperactive feeding, which can be partially restored through reconstitution of serotonin biosynthesis in only the ADF neurons (Figure 1B and Table S1 available online). Moreover, the extent of fasting-induced hyperactive feeding was reminiscent of the effects of treatment of well-fed animals with exogenous serotonin or serotonin reuptake inhibitors (Horvitz et al., 1982; Avery and Horvitz, 1990; Srinivasan et al., 2008). Serotonin-induced hyperactive feeding is dependent on the serotonergic GPCR, SER-5, and consequent inactivation of an AMP-activated kinase (AMPK) complex encoded by *aak-2* in a pair of interneurons that selectively express the obesity-associated transcription factor, Sim-1/HLH-34 (pathway summarized in Figure S1A) (Cunningham et al., 2012). Loss-of-function mutants of *ser-5* and *hlh-34* exhibited wild-type pumping rates during the ad-libitum-fed and -fasted states but failed to hyperactivate pumping post-fast (Figure 1B). Consistent with the notion that *aak-2* mutants mimic behaviors of animals with persistently elevated serotonin signaling, their already elevated feeding was not further elevated post-fast (Figure 1B).

To determine whether the observed changes in pumping rate correlated with changes in food ingestion, we assessed the accumulation of BODIPY dye within the intestines of wild-type, *tph-1*, *ser-5*, *hlh-34*, and *aak-2* mutants cultured on the food containing the fluorescent dye. There was a direct correlation between pumping rates of these strains and the extent of BODIPY accumulation (Figure S1B).

A Kynurenine Amino Transferase Functions Upstream of Serotonin to Regulate Feeding

Our findings suggested that, in the context of feeding regulation, serotonin signaling may exist in at least three states: (1) active

signaling in well-fed wild-type animals; (2) reduced signaling upon food removal, a condition mimicked by loss of *tph-1*; and (3) a transiently elevated serotonergic state post-fast, a condition mimicked by *aak-2* mutants. To understand the transient hyperactive pumping state better, we searched for additional mutants with altered pharyngeal pumping and found that *nkat-1(ok566)* loss-of-function mutants exhibited constitutively elevated pumping rates and food ingestion (Figures 2A and S1B). Similar to *aak-2* mutants, *nkat-1* mutants reduced their pharyngeal pumping upon fasting and had elevated feeding rate post-fasting that was not attenuated with continued feeding (Figure 2A). The hyperactive feeding of *nkat-1* deficiency was suppressed in *tph-1*, *ser-5*, and *hlh-34* mutants, whereas the elevated rates of *aak-2* mutants were not further changed by *nkat-1* deficiency (Figure 2B), suggesting that *nkat-1* can function upstream of serotonergic signaling.

NKAT-1 and two other *C. elegans* proteins (NKAT-3 and TATN-1) are homologous to mammalian kynurenine aminotransferases (KATs), which act on kynurenine (Kyn), a key intermediate of the kynurenine pathway (KP). In both *C. elegans* and mammals, Kyn is derived from the irreversible catabolism of tryptophan by tryptophan 2, 3 dioxygenase (Figure 2C). Depending on which enzymes then act on Kyn, it can have three distinct proximal metabolic fates. Kynurenine mono-oxygenase and kynureninase convert Kyn into 3-hydroxy kynurenine (3-Hkyn) and anthranilic acid (Ant), respectively, which are further transformed by other enzymes of the KP (Figure 2C) (van der Goot et al., 2012; Stipanuk and Caudill, 2013). Alternatively, as a substrate for KATs, kynurenine is oxidatively deaminated to form KynA, the only known biosynthetic route to this metabolite. To assess the role of KP metabolites in feeding behavior, we developed an HPLC-based assay to measure metabolite levels from whole-animal extracts. Mutants in *nkat-1* contained 50% less KynA than wild-type *C. elegans* fed ad libitum (Figure 2D). Levels of tryptophan and Kyn, the predicted substrate of *nkat-1*, were unchanged relative to wild-type animals, whereas levels of Ant were elevated in *nkat-1* mutants (Figure 2D). Other metabolites downstream of Kyn such a 3-hydroxykynurenine (3-HKyn, Figure 2C) or 3-hydroxyanthranilic acid (data not shown) were not detectable in either wild-type or *nkat-1* mutants in our assay. These findings suggested that NKAT-1 activity contributes to KynA pools and the deficiency in KAT activity may not significantly impact the organismal pool of Kyn substrate because it is 1,000-fold larger than that of KynA.

To determine whether the *nkat-1* pharyngeal pumping phenotype was related to its KynA deficiency, we supplemented the feeding media of *C. elegans* with either 0.1 or 2.5 mM KynA. These supplementations did not reduce the pharyngeal pumping rate of well-fed, wild-type animals on food (Figure 2E) but blocked the hyperactive feeding phenotype of *nkat-1* mutants (Figure 2E), indicating that a deficiency in KynA promotes hyperactive feeding.

KynA Levels Are Responsive to Fasting and Regulate Feeding

Because tryptophan is an essential amino acid in both *C. elegans* and vertebrates (van der Goot and Nollen, 2013), we suspected that nutrient status may affect the tissue pools of the KP metabolites. After 2 hr of fasting, both Kyn and KynA levels declined by 70%, but the decline of the levels of Trp, a 30- to 40-fold larger pool than that of Kyn, did not attain statistical significance, and levels of Ant increased by 40% (Figure 3A). Thus, fasting promotes degradation of kynurenine and a shift from production of KynA to that of Ant. During subsequent refeeding, levels of Kyn and KynA initially remained depressed, but then the levels of KynA and Ant recovered to their pre-fast, ad-libitum-fed state by 2 hr, the same time frame when animals attenuate their hyperactive feeding post-fast. Levels of Kyn at this time point still remained depressed (Figure 3A). As summarized in Figure 3B, these data indicated that, similar to serotonin signaling, KynA levels correlate with three distinct states of feeding behavior: (1) basal ad-libitum-fed state with normal levels of KynA, (2) a fasted state resulting in depressed KynA levels, and (3) a state of depressed KynA when animals encounter food immediately post-fast and exhibit hyperactive feeding. Given ample food supplies, animals in this state eventually return to the ad libitum feeding state.

To understand the influence of KynA in mediating the plasticity between feeding states, we altered KynA levels during different nutritional states. We supplemented basal medium with 100 μM of either Kyn (the physiological precursor to KynA), KynA, serotonin (5-HT), or 3-HKyn. These metabolite add backs were conducted during the fasting period and pharyngeal pumping rates were measured prior to and after animals were returned to food (Figure 3C). Consistent with the notion that a drop in serotonin signaling underlies the reduced feeding off of food, *C. elegans* treated with 5-HT during the 2 hr fast did not lower their feeding. Nevertheless, when these animals were returned to food (without added 5-HT), they still exhibited hyperactive feeding, indicating that the 5-HT signal of food availability is insufficient to mitigate the impact of fasting on post-fast feeding. Supplementations with KynA, but not Kyn, partially blocked the drop in pumping upon fasting (Figure 3C). Notably, both of these supplementations during the fasted state fully blocked the subsequent hyperactive state without affecting the rapid (within 1–2 min) rise in pumping from the low rates during fasting to the intermediate ad libitum rates upon exposure to food (Figures S2A and 3C). Treatment of fasting *C. elegans* with 3-HKyn, a metabolite irreversibly derived from Kyn and one that cannot be converted into KynA (Figure 2C), had no effects on feeding behavior during fasting or refeeding (Figure 3C). Metabolite measurements in fasting animals revealed that Kyn administration during fasting elevated KynA levels 3-fold over vehicle-treated animals, whereas levels of Kyn, Trp, or Ant were not significantly altered (Figure S2B).

We next examined the effects of kynurenine pathway mutations on KynA levels and feeding behavior. Under ad-libitum-fed conditions, levels of Kyn, KynA, and Ant were elevated 4- to 8-fold in *kmo-1(tm4529)* mutants relative to wild-type *C. elegans* (Figure S2C). Although subjecting the *kmo*-1 mutants to a 2 hr fast caused a decline in KynA levels, these levels still far exceeded that found in ad-libitum-fed wild-type animals (Figure S2C). The *kmo-1* mutants were unable to hyperactivate their pharyngeal pumping rate post-fast (Figure 3D). However, loss of *nkat-1* resulted in constitutively hyper-activated pharyngeal pumping, even in a *kmo-1* mutant background (Figure S2D).

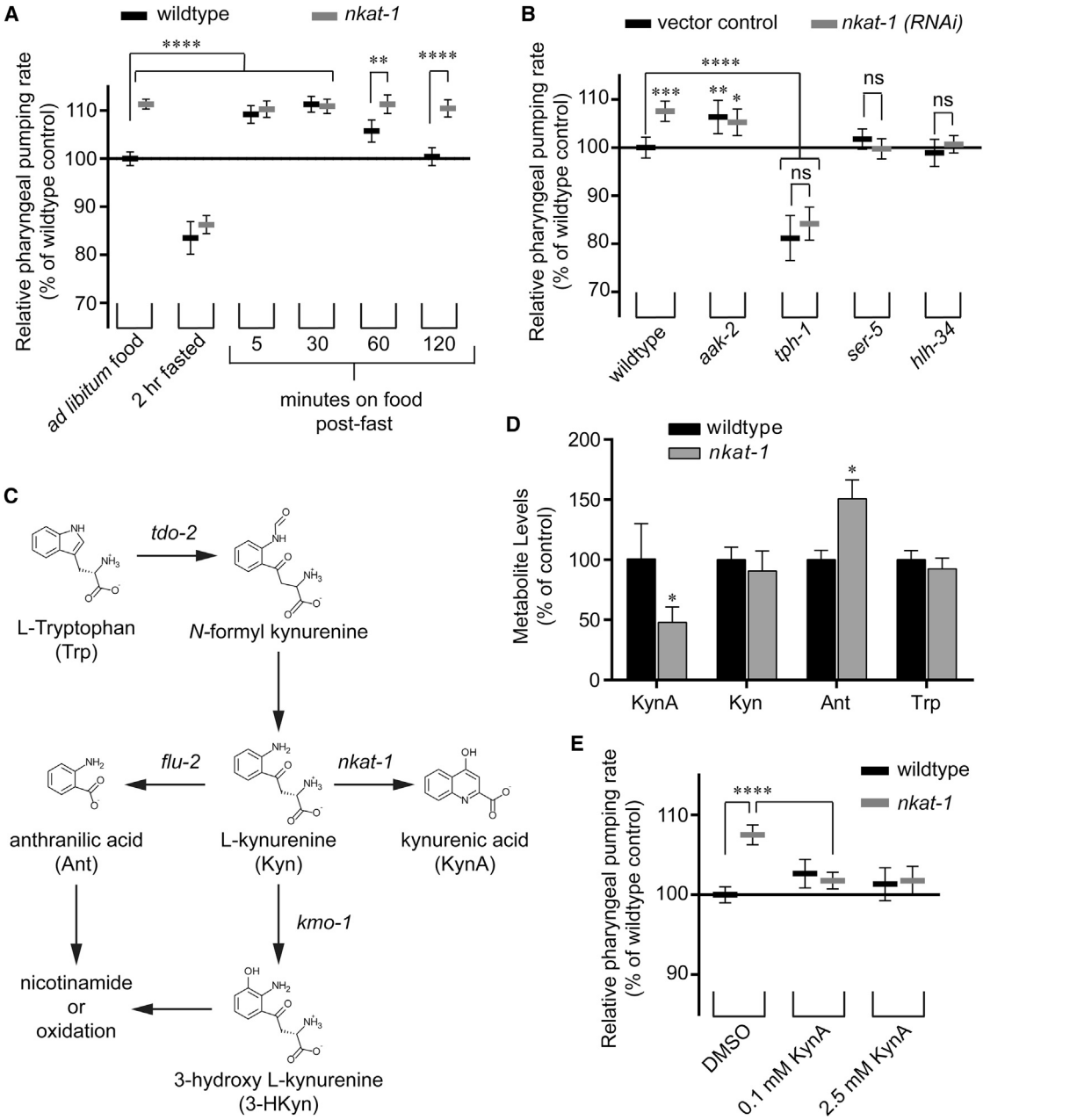

Figure 2. Mutants with Impaired KynA Production Exhibit Constitutively Hyperactive Pharyngeal Pumping that Requires Serotonin Signaling

(A) Pharyngeal pumping rates. n = 9–13 animals per condition. **p < 0.01 and ****p < 0.0001 ANOVA (Tukey).

(B) Pharyngeal pumping rates of serotonin pathway mutants cultured on either vector control RNAi or *nkat-1(RNAi)* expressing *E. coli*. n = 10 animals per condition. ns, p > 0.5, * p < 0.05, **p < 0.01, ***p < 0.001, and ****p < 0.0001 compared to wild-type animals cultured of RNAi control vector ANOVA (Dunnett).

(C) Schematic of the kynurenine pathway. *tdo-2*: tryptophan 2,3 dioxygenase; *kmo-1*: kynurenine mono-oxygenase; *flu-2*, required for kynureninase expression.

(D) Comparisons of kynurenine pathway metabolite levels in wild-type versus *nkat-1* mutants. Error bars indicate SD of determinations from five cultures per genotype. *$p < 10^{-5}$ (two-tailed, t test: wild-type versus *nkat-1*).

(E) Effects of KynA supplementation on pharyngeal pumping. n = 10 animals per condition. ****p < 0.0001 ANOVA (Tukey).

In (A), (B), and (E), error bars indicate 95% c.i.

Similar to *kmo-1* mutants, *flu-2(e1003)* mutants, which have low kynureninase activity and elevated Kyn and KynA levels (van der Goot et al., 2012), were unable to hyperactivate their pharyngeal pumping post-fast (Figure 3D).

Taken together, these results point to KynA as the specific metabolite whose levels determine the overfeeding behavior of animals post-fast; fasting results in a depression of KynA levels, which then permits the hyperactive feeding state when animals

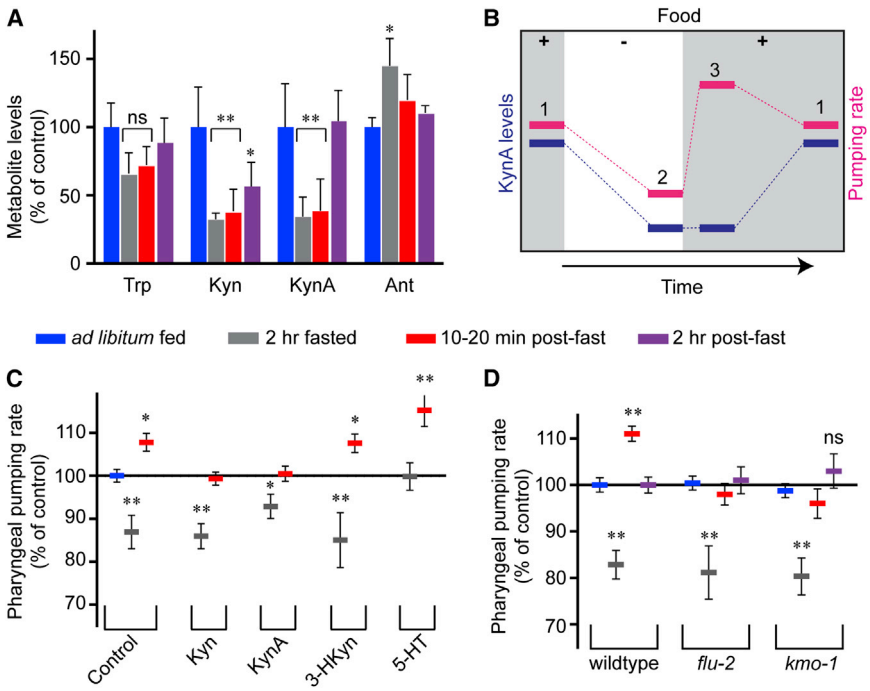

Figure 3. KynA Depletion during Fasting Is Required for Post-Fast Hyperactive Feeding

(A) Determination of tryptophan (Trp), kynurenine (Kyn), kynurenic acid (KynA), and anthranilic acid (Ant) from extracts of wild-type *C. elegans* fed ad libitum after 2 hr of fasting or after 20 min or 2 hr of post-fast feeding. For each metabolite, data are normalized to the ad-libitum-fed condition. Error bars indicate SD of three to four independent cultures. NS, $p > 0.05$, *$p < 0.05$, and **$p < 0.0001$. ANOVA (Tukey) relative to ad libitum fed for each metabolite.

(B) Observed relationships among KynA levels, pharyngeal pumping rate, and food availability with time indicating three distinct behavioral states (1–3).

(C) Effects of metabolite supplementations on pharyngeal pumping rates of wild-type *C. elegans*. During the fasting period, animals were treated with either vehicle or 100 μM of each of Kyn, KynA, 3-hydroxykynurenine (3-HKyn), and serotonin (5-HT). n = 10–12 animals per condition. ns, $p > 0.5$, *$p < 0.01$, and **$p < 0.0001$. ANOVA (Holm-Sidak) compared to ad-libitum-fed control.

(D) Pumping rates from wild-type and mutants at the indicated fasting and refeeding periods. n = 12–14 animals per condition. ns, $p > 0.05$ and **$p < 0.0001$. ANOVA (Holm-Sidak) compared to ad libitum fed for each mutant and wild-type control.

In (C) and (D), error bars indicate 95% c.i. See also Figure S2.

are returned to food. As food is ingested, KynA levels recover, attenuating the hyperactive feeding behavior.

Localized Production of KynA in the Nervous System Regulates Feeding

To identify the tissues of origin for KynA production, we generated transgenic animals expressing a transcriptional fusion of the *nkat-1* promoter to GFP (*nkat-1p::gfp*) and observed consistent expression in head neurons with occasional weak transgene expression in the gonad and intestine (Figure 4A). To identify the precise cells in which *nkat-1p::gfp* is expressed, we generated *nkat-1p*::*gfp; nmr-1p*::*mCherry* double transgenics (Figure 4B). The *nmr-1* promoter was previously shown to be expressed in NMDA receptor expressing neurons named AVA, AVE, AVD, PVC, AVG, and RIM (Brockie et al., 2001). Based on their axonal projections and cell body positions, two of the *nkat-1p* active neurons were identified as RMDV and RIM pairs of neurons, which are directly adjacent to *nmr-1*-expressing AVA and AVD neurons, respectively. Only sporadic, weak mCherry expression could be observed in RIM. The third *nkat-1p* active neuron situated dorsal to the nerve ring with an axon projection along the dorsal nerve cord was identified as RID. Thus, with the potential exception of RIM, *nkat-1* is likely expressed in neurons that lack NMDA receptors but are in close anatomical proximity to those that do (White et al., 1986).

Reconstitution of the *nkat-1* cDNA using the *nkat-1* promoter described above, a pan-neuronal promoter (*unc-119*) or its selective expression in only the RIM and RIC interneurons using the *tdc-1* promoter, completely rescued the hyperactive pumping phenotype of *nkat-1* mutants (Figure 4C). By contrast, *nkat-1* mutants continued to exhibit hyperactive feeding when *nkat-1* cDNA was reconstituted either in the ADF serotonergic neurons using the *srh-142* promoter or when using the *nkat-3* promoter, which is robustly expressed in pharyngeal muscle, as well as in some head neurons (Figures S3A and S3B). Thus, production of KynA at specific neural locations is a critical determinant of feeding behavior.

A Neuropeptide Signaling Axis Emanating from NMDA-R-Expressing Interneurons Regulates Post-Fast Hyperactive Feeding

In mammals, KynA has been characterized as an antagonist of glutamatergic neurotransmission in particular through NMDA-gated ionotropic receptors (Perkins and Stone, 1982) and by presynaptic inhibition of glutamate release via antagonism of α-7 nicotinic acetylcholine receptors (Carpenedo et al., 2001). The spatial expression patterns of *nkat-1* and *nmr-1* prompted us to investigate the role of *C. elegans* NMDA-receptor (NMDA-r) in feeding behavior. The two subunits of the *C. elegans* NMDA-r are encoded by *nmr-1* and *nmr-2*, which have identical expression patterns in a few interneurons (Brockie et al., 2001). Both *nmr-1(ak4)* and *nmr-2(tm3785)* loss-of-function mutants exhibited pharyngeal pumping rates indistinguishable from wild-type animals when fed ad libitum and while fasting (Figures 5A and 5B). However, both mutants were insensitive to the feeding increasing effects of *nkat-1* deficiency (Figure 5A) and failed to exhibit post-fast hyperactive feeding (Figure 5B). Expression of the *nmr-1* cDNA under the control of the *nmr-1* promoter restored the capacity for hyperactive feeding (Figures S4A and S4B). Unlike the case of the *nkat-1* phenotypic rescue,

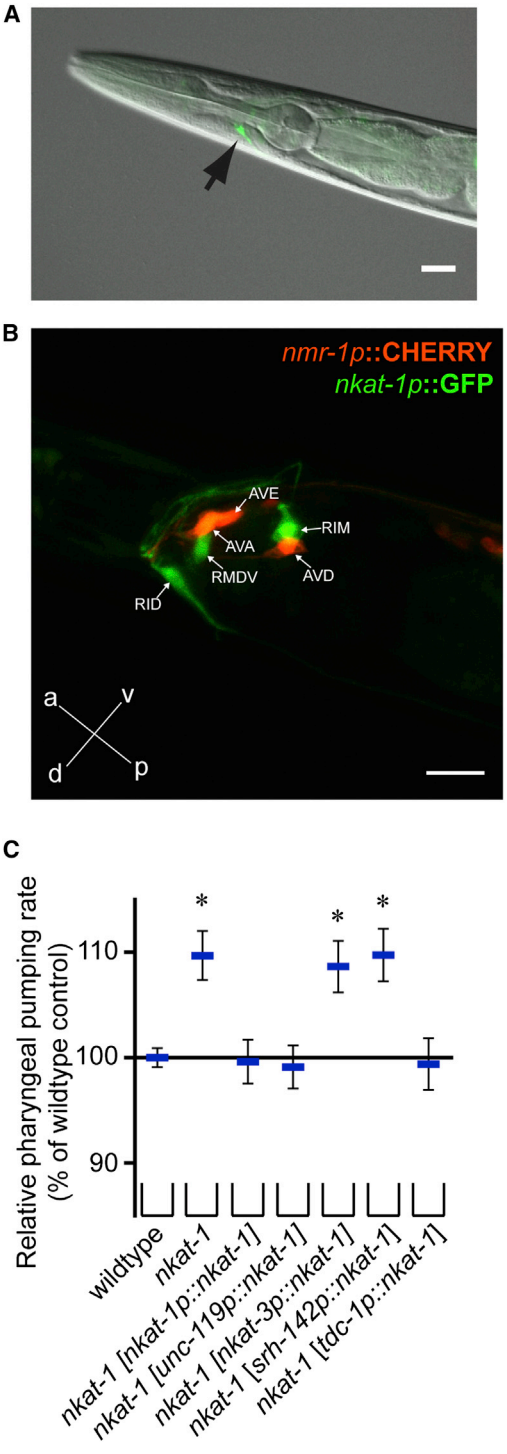

Figure 4. *nkat-1* Expression Is Limited to a Few Neurons

(A) Merged DIC and green epifluorescence image of an animal containing an *nkat-1p::gfp* transcriptional fusion. Arrow indicates a green head neuron. Scale bar, 20 μm.

(B) Maximum intensity projection of the right lateral side of the head of a young adult animal coexpressing *nkat-1p::gfp* and *nmr-1p::mCherry* transcriptional fusions. Individual neurons are identified. Scale bar, 10 μm.

(C) Pharyngeal pumping rates of the indicated strains. Error bars indicate 95% c.i. n = 10–12 animals per condition. ****p < 0.0001 ANOVA (Dunnett) in comparison with wild-type.

See also Figure S3 and Table S1.

expression of *nmr-1* cDNA in RIM and RIC using the *tdc-1* promoter or in RIM alone using the *cex-1* promoter (Cohen et al., 2009) was insufficient to rescue the hyperactive feeding defect of *nmr-1* mutants (Figures S4A and S4B). Moreover, although *nmr-1(RNAi)* suppressed the hyperactive feeding state of *nkat-1* mutants, it failed to alter the constitutive depressed pumping of serotonin deficient *tph-1* mutants or the hyperactive pumping of AMPK deficient *aak-2* mutants (Figure S4C). Collectively, our data suggested a model whereby KynA levels modulate the feeding rate by directly or indirectly antagonizing glutamatergic neurotransmission through NMDA-r and subsequent changes in serotonin signaling initiated from the ADF neurons.

To substantiate the above model, we searched for molecular links between NMDA-receptor-expressing neurons and serotonin signaling by examining neurotransmitter or neuropeptide pathways of *nmr-1*-positive neurons. The hyperactive feeding of *nkat-1*-deficient animals was unaltered in *tdc-1* mutants, which are deficient in the production of tyramine and octopamine, feeding regulatory neurotransmitters originating from the RIM and RIC interneurons, respectively (Figure 5C) (Alkema et al., 2005; Greer et al., 2008). Similarly, elevated feeding of *nkat-1*-deficient animals was not dependent on *flp-1* (an FMFRamide neuropeptide), whose expression includes *nmr-1*-positive AVA and AVE neurons and has been previously implicated in serotonin-regulated behaviors (Waggoner et al., 2000) (Figure 5C). However, loss of *flp-18*, which is expressed in AVA, RIM, and four other neurons and regulates fat metabolism, chemotaxis, and movement (Cohen et al., 2009), blocked the hyperactive feeding of *nkat-1*-deficient animals and the post-fast hyperactive feeding of wild-type animals (Figures 5C and 5D) without affecting ad libitum feeding rates. Reconstitution of *flp-18* using the *nmr-1* promoter was sufficient to rescue hyperactive feeding induced by *nkat-1* inactivation (Figure 5C) or fasting (Figure 5D), whereas reconstitutions in AIY (*ttx-3* promoter) (Altun-Gultekin et al., 2001) and in RIM alone (*cex-1* promoter) failed to do so (Figures 5C and 5D). Because the only neurons that overlap between expression patterns of *flp-18* and *nmr-1* are AVA and RIM, and RIM-specific expression of *flp-18* and *nmr-1* was insufficient to restore post-fast hyperactive feeding state to their respective mutants, AVA remains as the likely origin of the *flp-18* signal required for hyperactive feeding. Promoters for exclusive expression in AVA are not yet known.

The FLP-18 neuropeptide activates two different receptors, NPR-4 and NPR-5, that are related to the mammalian neuropeptide-Y receptor (Kubiak et al., 2008; Cohen et al., 2009). The two receptors have nonoverlapping expression with NPR-5 being expressed in select sensory neurons, including serotonergic ADF (Cohen et al., 2009). Similar to *nmr-1* and *flp-18* mutants, *npr-5* mutants have wild-type pharyngeal pumping rates when feeding ad libitum and when fasted but do not hyperactivate pharyngeal pumping in response to *nkat-1* deficiency (Figure 5E) or post-fast food encounter (Figures 5F and S4D). Transgenic expression of *npr-5* (a and b isoforms) solely in the ADF sensory neuron was

sufficient rescue the feeding deficiencies of *npr-5* mutants (Figures 5E and 5F). Finally, unlike its requirement in the case of *nkat-1* deficiency, loss of *npr-5* does not alter the constitutively hyperactivated feeding of *aak-2* mutants (Figure S4E). These results suggest that KynA depletion impinges on serotonin in ADF by an NMDA-r to FLP-18 to NPR-5 signaling axis.

Fasting Enhanced Activity in AVA Interneurons Is Repressed by KynA, Requires NMDA-r, and Is Independent of FLP-18

The prior results implied that the fasted state in *C. elegans* is sensed at least in part by the loss of KynA-mediated antagonism of NMDA-receptor-expressing interneurons. To measure the effect of varying KynA levels on the activity of *nmr-1*-expressing neurons, we measured calcium transients in these neurons using the intensity ratio of the fluorescent Ca^{2+} indicator GCaMP3 (Tian et al., 2009) and the Ca^{2+}-insensitive mCherry both expressed under the control of the *nmr-1* promoter. The *nmr-1p::GCaMP3*, *nmr-1p::mCherry* transgenes did not alter feeding rate of animals under any of the tested conditions (Figure S5). Because the depletion of KynA caused by fasting or genetic inactivation of *nkat-1* is a chronic condition, we measured spontaneous Ca^{2+}-induced fluorescence transients over an extended (250 s) period. The *nmr-1* promoter used to drive GCaMP3 had the most prominent expression in the AVA neurons; however, with our optical setup, we cannot rule out the acquisition GCaMP signal from both AVA and AVE. For all of our analyses, we report the total integrated signal of all the peaks in the 250 s recording window (Figures 6A and 6B). To enable comparisons of the average intensities and durations of the spontaneous, stochastic Ca^{2+} transients under different conditions, we also examined each of the 250 s recording windows for events where we could unambiguously define initiation of a spontaneous transient. We then plotted GCaMP fluorescence for the following 60 s (Figure 6A) and examined the average response of multiple such transients per condition (Figure 6C).

The total integrated change in fluorescence intensity was 2.5-fold larger in fasted wild-type animals than in fed animals (Figure 6B). Examination of the transients in the 60 s window following an initiation event indicated that the enhanced intensity observed during fasting persisted throughout the evaluation window rather than reflecting a series of short but very intense bursts of the Ca^{2+} signal (Figure 6C). Kyn or KynA supplementations reverted the elevated integrated intensity Ca^{2+} signal of fasted animals to that of ad-libitum-fed animals (Figure 6B). These supplementations did not block the initial intensity maximum of spontaneous Ca^{2+} transients in fasted animals but promoted their rapid decline to levels comparable to or below that of fed wild-type animals (Figure 6C).

Under ad-libitum-fed conditions, the total integrated fluorescence signal, as well as the size and duration of the Ca^{2+} transients of *nkat-1* mutants, was greater than those of ad-libitum-fed wild-type animals and comparable to those of fasted wild-type animals (Figures 6B and 6C). Although the total integrated intensity of GCaMP fluorescence was statistically indistinguishable between wild-type and *nmr-1* mutants during the well-fed state (Figure 6B), loss of *nmr-1* abrogated the fasting-induced elevation of total integrated response (Figure 6B) and the persistent rise in transients (Figure 6C). These results are consistent with kynurenic acid attenuating NMDA-receptor-mediated Ca^{2+} activity in the ad-libitum-fed state, which is relieved upon fasting in wild-type animals or in animals deficient in *nkat-1* function.

We also found that the total integrated intensity (Figure 6B) and duration of Ca^{2+} transients (Figure 6C) that occur upon fasting were similar in *flp-18* mutants and wild-type animals. This suggested that the requirement for *flp-18* in post-fast hyperactive feeding is not merely an indirect outcome of inability of AVA neurons to respond to fasting in *flp-18* mutants. Although loss of *flp-18* did not alter the total integrated intensity of Ca^{2+} transients during the fed state, we noted that the intensity of these transients was more elevated relative to those of fed wild-type animals when they occurred (Figure 6C). The reasons for this are not known but may reflect a paracrine or autocrine feedback inhibitory action of FLP-18 on the activity of AVA.

KynA Levels Regulate the Amount of Secretion from ADF in Response to Food through FLP-18/NPR-5 Signaling

Because the transition from the slow-pumping fasted state to the hyperactivated post-fast state occurs within minutes (Figure S2A), we surmised that it could be driven by changes in secretion of serotonin from ADF, a process with a fast response capability (Whim and Moss, 2001). Direct observation of serotonin secretion is challenging. Both serotonin and neuropeptides such as DAF-28, an insulin-like peptide (Li et al., 2003), are secreted via dense-core vesicles. As a proxy for serotonin secretory activity, we measured the secretion of a DAF-28::mCHERRY translational fusion from ADF using a previously established assay (Kao et al., 2007; Lee et al., 2011). Depletion of KynA caused by *nkat-1* deficiency resulted in enhanced secretion of the reporter, which was completely abrogated in both *flp-18* and *npr-5* mutants (Figure 6D). Similarly, wild-type, but not *flp-18* or *npr-5* mutant, animals that had been fasted and returned to food for 20 min exhibited enhanced secretion compared to ad-libitum-fed animals (Figure 6E). Animals that had simply been fasted for 2 hr without subsequent food exposure exhibited no significant change in secretion (Figure 6E).

DISCUSSION

We have identified KynA as part of a whole-organism homeostatic feedback loop that allows animals to gauge whether they have experienced a period of fasting to alter subsequent feeding behavior (Figure 7). Because KynA is derived from tryptophan, an essential amino acid, changes in KynA levels are metabolically linked to nutritional status. Our findings suggest a model whereby fasting depletes KynA, leading to activation of NMDA-receptor-expressing neurons, which is consistent with the known role of KynA as an inhibitor of NMDA signaling. In turn, activation of these neurons initiates a neuropeptide Y-like signaling cascade, comprised of FLP-18 and its receptor NPR-5, that poises the ciliated ADF neurons for enhanced secretion of serotonin as soon as they sense the presence of

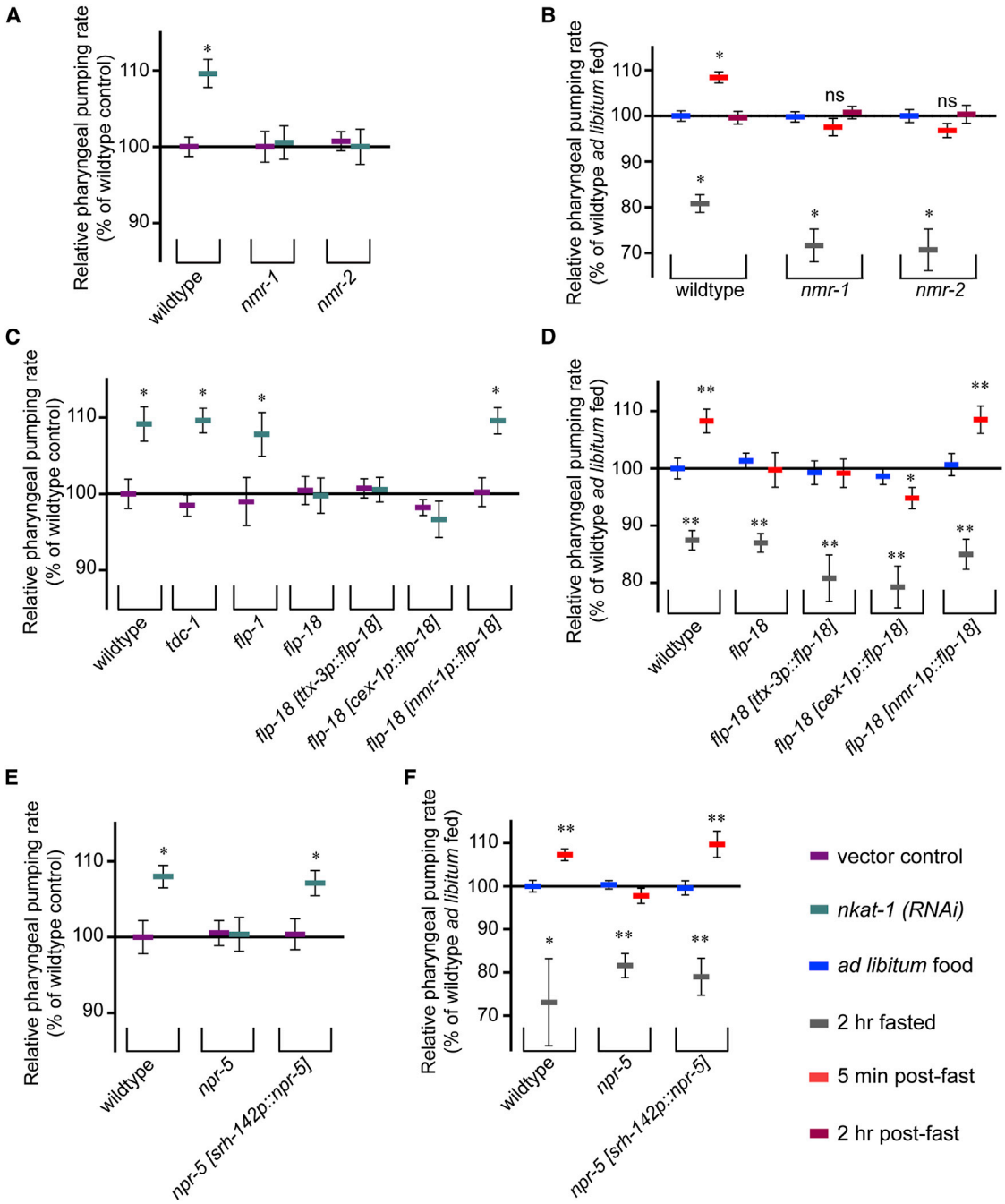

Figure 5. Hyperactive Feeding Requires an NMDA Receptor to Peptidergic Signaling Axis that Converges on a Serotonergic Sensory Neuron

(A) Pharyngeal pumping rates of wild-type, *nmr-1*, and *nmr-2* mutants cultured on either RNAi vector control or *nkat-1(RNAi)*. *p < 0.0001, ANOVA (Tukey).

(B) Pharyngeal pumping rates at the indicated fasting and refeeding periods. ns, p > 0.1 and *p < 0.0001. ANOVA (Tukey) comparing fasted, post-fast animals to ad-libitum-fed controls.

(C) Pharyngeal pumping rates of the indicated strains. Animals were cultured on bacteria expressing *nkat-1(RNAi)* or RNAi vector control. *p < 0.0001 ANOVA (Sidak) comparing vector control to *nkat-1(RNAi)* for each genotype.

(D) Pharyngeal pumping rates of wild-type, *flp-18* mutants, and *flp-18* transgenic lines used in (C) fed ad libitum, after 2 hr of fasting, and after 5 min of post-fast refeeding. *p < 0.05 and **p < 0.0001. ANOVA (Tukey) comparing fasting and post-fast measurements to that of ad libitum fed for each measurement.

(E) Pharyngeal pumping rates of wild-type, *npr-5* mutants, and *npr-5* mutants expressing transgenes directing expression of *npr-5a* and *-5b* to ADF neurons. Animals were cultured on bacteria expressing either RNAi vector control or *nkat-1(RNAi)*. *p < 0.0001. ANOVA (Sidak) comparing vector control treated to *nkat-1(RNAi)* treated for each genotype.

(legend continued on next page)

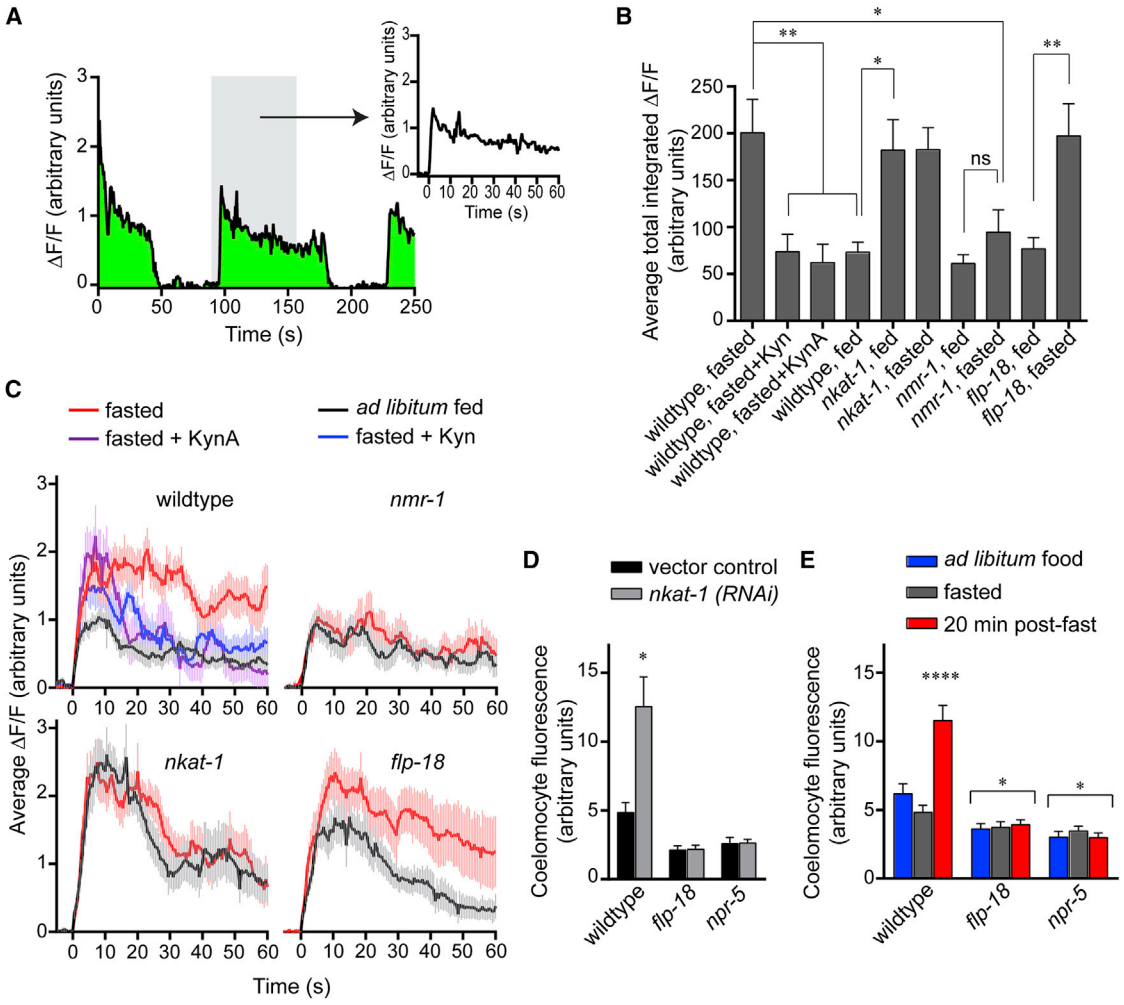

Figure 6. KynA Represses AVA Interneuron Activity and Secretion from ADF through Antagonism of the NMDA-r/FLP-18/NPR-5 Signaling Axis

(A) Sample ratiometric ΔF/F plot showing spontaneous changes over the 250 s imaging window. The area under the signal in the green shaded plot is the basis of the data in (B). The inset plot shows the portion of a spontaneous transient extracted from the 250 s imaging window aligned to a −5 to 60 s time-scale axis, which is the basis of the data shown in (C). See also Figure S5.

(B) The total integrated change in fluorescence intensity (ΔF/F) over the 250 s recordings. Wild-type animals were fed ad libitum, fasted 2 hr, or fasted 2 hr in media supplemented with either 100 μM Kyn or 100 μM KynA. Mutants in *nkat-1*, *nmr-1*, and *flp-18* were fed ad libitum or fasted 2 hr. ns, $p > 0.8$, $^{*}p < 0.02$, and $^{**}p < 0.01$; ANOVA (Sidak).

(C) Averaged spontaneous Ca^{2+} transients from each of the conditions recorded in (B). (B and C) error bars indicate SEM; n = 10–12 animals per condition.

(D and E) Measurement of DAF-28::MCHERRY fluorescence in coelomocytes from transgenic animals expressing *daf-28::mCherry* in ADF neurons. Error bars indicate SEM; n = 15–38 per condition.

(D) Wild-type, *flp-18*, and *npr-5* mutants expressing the transgene were cultured on bacteria expressing either *nkat-1(RNAi)* or an RNAi vector control. $^{*}p < 0.0001$ ANOVA (Tukey) compared to RNAi vector control-treated animals.

(E) Lines used in (D) measured during ad libitum feeding after a 2 hr fast and after 20 min of post-fast refeeding. $^{*}p < 0.05$ and $^{****}p < 0.0001$. ANOVA (Dunnett) comparing all measurements to wild-type, ad-libitum-fed animals.

food. The elevated serotonin signaling promotes enhanced feeding by the animals through a previously described pathway (Cunningham et al., 2012). As animals feed, the activity of NMDA-receptor-expressing neurons is attenuated by normalizing levels of KynA, which decreases FLP-18 to NPR-5 signaling in ADF, and terminates the transiently enhanced

(F) Pharyngeal pumping rates of wild-type, *npr-5* mutants, and the *npr-5* transgenic line used in (E) fed ad libitum, after 2 hr of fasting, and after 5 min of refeeding post-fast. $^{*}p < 0.05$ and $^{**}p < 0.0001$. ANOVA (Tukey) comparing fasting and post-fast measurements to that of ad libitum fed for each measurement.

In (A–F), error bars indicate 95% c.i. n = 10–16 animals per condition. See also Figure S4 and Table S1.

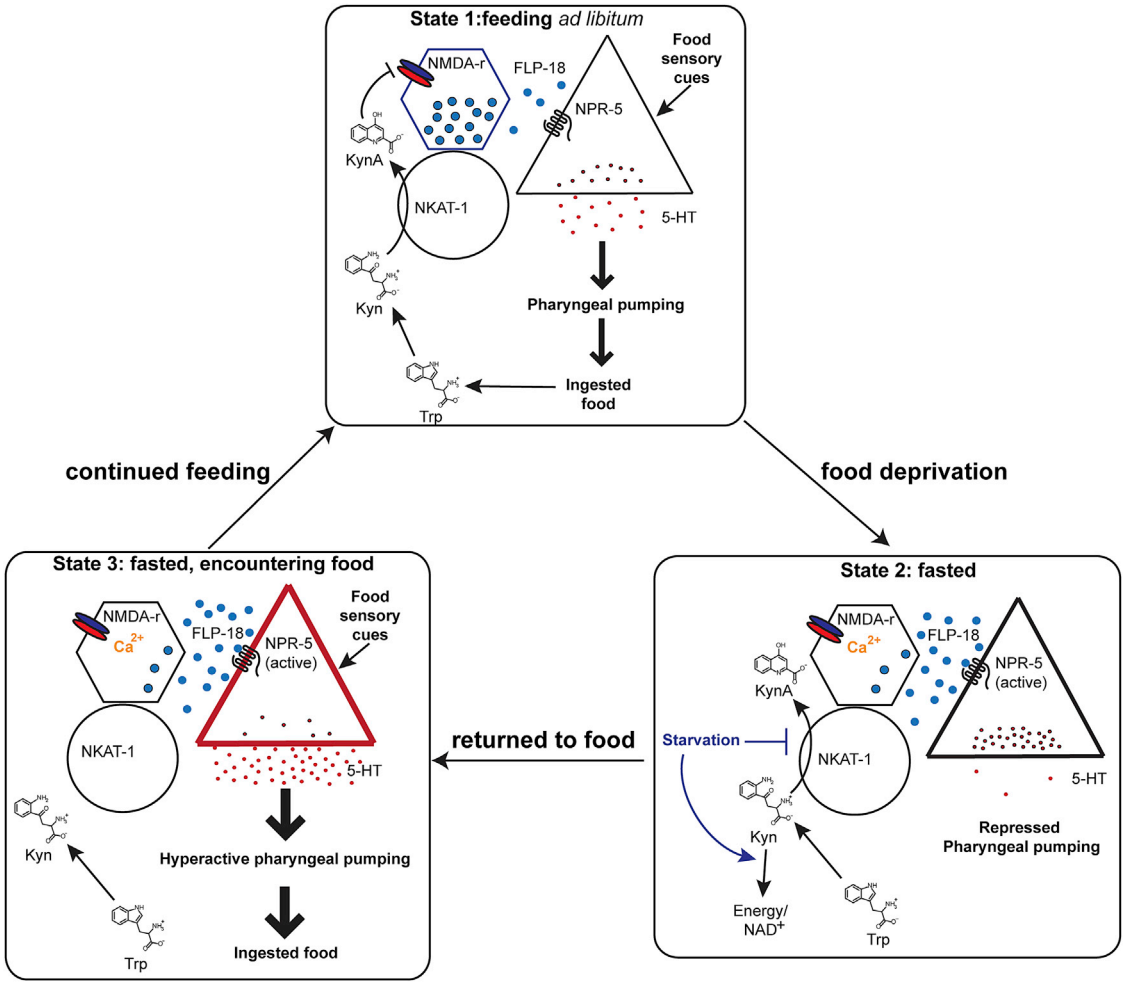

Figure 7. Model of a Neural Circuit that Integrates Food Sensory Cues with Nutritional Status to Promote Experience-Dependent Plasticity of Feeding

State 1: the activity of AVA (hexagon) is attenuated by KynA synthesized from kynurenine by NKAT-1 in RIM, RMDV, and/or RID (circle). Kynurenine is ultimately derived from ingested food. ADF (triangle) senses food cues leading to 5-HT secretion to stimulate pumping. State 2: fasting represses KynA production, causing activation of AVA neurons that promotes FLP-18/NPR-5 signaling to serotonergic ADF. In the absence of food cues, serotonin signaling from ADF is muted. State 3: when animals re-encounter food immediately post-fast, the activated NPR-5 signaling state leads to enhanced secretion from ADF when food derived sensory cues are detected. Continued feeding leads to an accumulation of KynA returning the animals to *State 1*.

serotonin signaling phase. This regulatory logic is analogous to a classical product feedback inhibition loop but one that acts on an entire neural circuit. This circuit does not simply inform the animals of the presence or absence of food but allows animals to alter behaviors in a manner that takes into account an internal nutritional cue modulated by fasting.

Although tryptophan degradation via the KP likely occurs throughout the animal (van der Goot et al., 2012), we found that the highly restricted expression pattern for *nkat-1* in the nervous system in the close spatial proximity of NMDA-receptor-expressing neurons was critical to its function in feeding behavior. Kynurenic acid is thought to antagonize glutamate signaling through binding extracellular motifs of cell-surface receptors such as the glycine coagonist site on NMDA receptors or α-7 nAChRs. Either mechanism would be consistent with our genetic data. In mammals, because it does not cross the blood-brain barrier, KynA in the brain is synthesized by astrocytic KATs (Schwarcz et al., 2012). Therefore KynA functions cell nonautonomously. In *C. elegans*, *nkat-1* is expressed in three sets of neurons: RID, RMDV, and RIM, of which reconstitution of *nkat-1* in RIM was sufficient to confer wild-type feeding behavior to *nkat-1* mutants. The cell bodies of RMDV lie directly adjacent to those of NMDA-receptor-expressing AVA, whereas the processes of AVA and RIM are closely associated, forming several gap junctions in the nerve ring (White et al., 1986). Thus, KynA produced by NKAT-1 in RIM and RMDV is in close spatial proximity for influencing glutamate signaling in AVA and other NMDA-r-expressing neurons. A controversy in how KynA regulates mammalian glutamatergic signaling stems from the fact that the K_i of KynA for NMDA and AMPA type glutamate receptors is 10- and 100-fold higher, respectively, than the concentration of KynA measured in the bulk

extracellular space (Albuquerque and Schwarcz, 2013). However, it is possible that the concentration of KynA increases dramatically in the microscopic vicinity of a cell competent to synthesize it. Heterogeneous, localized production of KynA may differentially modulate glutamatergic signaling in different brain regions or local synaptic clusters.

Our findings suggested that FLP-18 originating from AVA neurons during the fasted state acts on the ADF food-sensing neurons via NPR-5, an ortholog of the mammalian neuropeptide-y (NPY) receptors, to increase food consumption post-fast. The AVA interneuron is also required for and its activity is correlated with initiating spontaneous reversals, a locomotory behavior that is increased in the absence of food (Gray et al., 2005; Piggott et al., 2011). Thus, AVA neurons direct two distinct functional outputs coordinated to rectify the aversive fasted state: food seeking behavior and food ingestion. This is not likely a consequence of the relatively simple nature of the *C. elegans* nervous system. For example, in mice, starvation induced activation of AgRP neurons in the hypothalamus, which also express NPY, and elicited both food-seeking behavior and elevated consumption of food through projections within the hypothalamus and to the midbrain (Betley et al., 2013). AgRP neurons also express NMDA receptors and targeted genetic ablation of NMDA receptors in AgRP neurons, attenuates the post-fast hyperphagia in mice (Liu et al., 2012). Thus, AgRP neurons represent a prime point of control in mammals upon which KynA inhibition of glutamate signaling could play a role in food-associated behaviors.

The nervous system can gauge peripheral metabolic status by direct sensation of circulating nutrients such as glucose, leucine, or lipids, as well as through indirect hormonal pathways that originate from peripheral organs and signal to the nervous system (Lam, 2010). As an indicator of nutrient status, KynA stands out because it appears to directly modulate synaptic transmission, akin to a neurotransmitter whose levels are directly tied to nutrient availability. As recently exemplified (Agudelo et al., 2014), changes in peripheral metabolism can exert effects on central KP metabolite levels. Because defects in peripheral metabolic regulation are associated with a diverse array of CNS-associated diseases (Cai et al., 2012; Mitchell et al., 2013; McElroy and Keck, 2014), KynA presents an intriguing possibility for directly linking metabolism to various neural functions. Additionally, our findings provoke a possible twist in the interpretation of the serotonin-kynurenine hypothesis of depression in that KP activation may indeed antagonize serotonin—not through direct metabolic competition for their common precursor as previously proposed (Lapin and Oxenkrug, 1969) but through the production of KynA and its antagonism of a neural circuit that, in turn, enhances serotonin release. In the case of neurodegenerative disorders, the beneficial effects of KynA have been attributed to its potential for countering glutamate toxicity (Schwarcz et al., 2012). Another possibility raised by our studies is that the effects of KynA may be due to modulation of neural circuits whose normal, physiological functions may have beneficial impacts on proteostasis and neurodegeneration. In *C. elegans*, serotonin signaling, which we show is attenuated by KynA, regulates release of systemic neuroendocrine molecules, including insulin (Cunningham et al., 2014; Liang et al., 2006), a well-known modulator of proteostasis (Taylor et al., 2014).

EXPERIMENTAL PROCEDURES

Please see Extended Experimental Procedures for detailed procedures.

C. elegans Strains

Transgenic lines were prepared by microinjection of expression plasmids. Unless described otherwise, *C. elegans* were cultured on agar plates at 20°C on *E. coli* OP-50.

Materials

Unless described otherwise, all chemicals were purchased from Sigma. Plasmids were constructed using standard molecular biology techniques.

Pharyngeal Pumping Assay

The number of contractions of the posterior pharyngeal bulb was counted over 10 s intervals as described (Srinivasan et al., 2008). All pumping rates presented in this study are presented in tabular form in Data S1.

BODIPY Uptake Assay

C. elegans were added to plates containing BODIPY (200 ng/ml) and *E. coli* for 15 min, washed off, paralyzed with NaN_3, and imaged (You et al., 2008).

Metabolite Determination

Acidified, aqueous extracts of *C. elegans* cultures were separated using an HPLC equipped with a 150 × 4.6 mm C_{18}-reversed phase column operating at flow rate of 1 ml/min. Metabolites were detected using in-line fluorescence and UV absorbance detectors. Retention times and excitation/emission data were compared to that of metabolite standards injected under the same conditions.

Metabolite Supplementation

Day 1 gravid adults were washed free of bacteria and then incubated for 2 hr in S-basal media supplemented with metabolites at 100 μM concentration. Ad libitum feeding: L4 animals were cultured for 1 day on plates containing 0.1 or 2.5 mM KynA.

Spontaneous Ca^{2+} Transients

Animals were mounted on agarose pads, immobilized with coverslips, and imaged for 250 s through a 40× objective on a microscope equipped with green and red epifluorescence filters and with a 16-bit camera acquiring 4 × 4 binned images on two channels sequentially at 2 Hz. A 6 × 6 pixel region of interest was placed over AVA, and the integrated fluorescence intensity at each time point for both the GCaMP signal and mCherry signal was measured. The Ca^{2+} signal was determined by normalizing the green channel by the red channel measurements for each time point.

Secretion Assay

The integrated fluorescence intensity from the red channel was measured in coelomocytes from animals that expressed the DAF-28::MCHERRY fusion protein from neuron-specific promoters using ImageJ.

Statistics

Two-tailed Student's t tests were used to calculate p values when comparisons were limited that between two conditions. When multiple conditions were compared per experiment, one or two-way ANOVA with appropriate post-tests was used to calculate p values.

SUPPLEMENTAL INFORMATION

Supplemental Information includes Extended Experimental Procedures, five figures, one data file, and one table and can be found with this article online at http://dx.doi.org/10.1016/j.cell.2014.12.028.

AUTHOR CONTRIBUTIONS

G.A.L., K.A.C., and K.A. designed experiments. G.A.L. and K.A.C. performed experiments. L.L. and F.M. provided technical assistance. G.A.L., K.A.C., Z.W., and K.A. analyzed data. G.A.L. and K.A. wrote the manuscript.

ACKNOWLEDGMENTS

The authors thank Shao-Yi Huang, Paul Muchowski, Steve Finkbeiner, Mihir Vohra, and Erik Johnson for helpful discussions and shared equipment and the Nikon Imaging Center at UCSF for microscope access. Some *C. elegans* strains were provided by the *Caenorhabditis* Genetics Center, funded by NIH Office of Research Infrastructure Programs (P40 OD010440), and the Mitani Lab of the National Bioresource Project of Japan for the Experimental Animal *C. elegans*. This research was supported by funds from the Program in Breakthrough Biomedical Research, UCSF Diabetes Family Fund for Innovative Patient Care, R21 ES021412 (NIEHS), R01 AG046400 (NIA), and U01 ES019458 (NCI).

Received: June 19, 2014
Revised: October 16, 2014
Accepted: December 11, 2014
Published: January 15, 2015

REFERENCES

Agudelo, L.Z., Femenía, T., Orhan, F., Porsmyr-Palmertz, M., Goiny, M., Martinez-Redondo, V., Correia, J.C., Izadi, M., Bhat, M., Schuppe-Koistinen, I., et al. (2014). Skeletal muscle PGC-1α1 modulates kynurenine metabolism and mediates resilience to stress-induced depression. Cell *159*, 33–45.

Albuquerque, E.X., and Schwarcz, R. (2013). Kynurenic acid as an antagonist of α7 nicotinic acetylcholine receptors in the brain: facts and challenges. Biochem. Pharmacol. *85*, 1027–1032.

Alkema, M.J., Hunter-Ensor, M., Ringstad, N., and Horvitz, H.R. (2005). Tyramine Functions independently of octopamine in the Caenorhabditis elegans nervous system. Neuron *46*, 247–260.

Altun-Gultekin, Z., Andachi, Y., Tsalik, E.L., Pilgrim, D., Kohara, Y., and Hobert, O. (2001). A regulatory cascade of three homeobox genes, ceh-10, ttx-3 and ceh-23, controls cell fate specification of a defined interneuron class in C. elegans. Development *128*, 1951–1969.

Andiné, P., Lehmann, A., Ellrén, K., Wennberg, E., Kjellmer, I., Nielsen, T., and Hagberg, H. (1988). The excitatory amino acid antagonist kynurenic acid administered after hypoxic-ischemia in neonatal rats offers neuroprotection. Neurosci. Lett. *90*, 208–212.

Avery, L., and Horvitz, H.R. (1990). Effects of starvation and neuroactive drugs on feeding in Caenorhabditis elegans. J. Exp. Zool. *253*, 263–270.

Avery, L., and You, Y.J. (2012). C. elegans feeding. WormBook, 1–23.

Beal, M.F., Matson, W.R., Storey, E., Milbury, P., Ryan, E.A., Ogawa, T., and Bird, E.D. (1992). Kynurenic acid concentrations are reduced in Huntington's disease cerebral cortex. J. Neurol. Sci. *108*, 80–87.

Betley, J.N., Cao, Z.F.H., Ritola, K.D., and Sternson, S.M. (2013). Parallel, redundant circuit organization for homeostatic control of feeding behavior. Cell *155*, 1337–1350.

Brockie, P.J., Mellem, J.E., Hills, T., Madsen, D.M., and Maricq, A.V. (2001). The C. elegans glutamate receptor subunit NMR-1 is required for slow NMDA-activated currents that regulate reversal frequency during locomotion. Neuron *31*, 617–630.

Cai, H., Cong, W.N., Ji, S., Rothman, S., Maudsley, S., and Martin, B. (2012). Metabolic dysfunction in Alzheimer's disease and related neurodegenerative disorders. Curr. Alzheimer Res. *9*, 5–17.

Campesan, S., Green, E.W., Breda, C., Sathyasaikumar, K.V., Muchowski, P.J., Schwarcz, R., Kyriacou, C.P., and Giorgini, F. (2011). The kynurenine pathway modulates neurodegeneration in a Drosophila model of Huntington's disease. Curr. Biol. *21*, 961–966.

Carpenedo, R., Pittaluga, A., Cozzi, A., Attucci, S., Galli, A., Raiteri, M., and Moroni, F. (2001). Presynaptic kynurenate-sensitive receptors inhibit glutamate release. Eur. J. Neurosci. *13*, 2141–2147.

Cohen, M., Reale, V., Olofsson, B., Knights, A., Evans, P., and de Bono, M. (2009). Coordinated regulation of foraging and metabolism in C. elegans by RFamide neuropeptide signaling. Cell Metab. *9*, 375–385.

Cunningham, K.A., Hua, Z., Srinivasan, S., Liu, J., Lee, B.H., Edwards, R.H., and Ashrafi, K. (2012). AMP-activated kinase links serotonergic signaling to glutamate release for regulation of feeding behavior in C. elegans. Cell Metab. *16*, 113–121.

Cunningham, K.A., Bouagnon, A.D., Barros, A.G., Lin, L., Malard, L., Romano-Silva, M.A., and Ashrafi, K. (2014). Loss of a neural AMP-activated kinase mimics the effects of elevated serotonin on fat, movement, and hormonal secretions. PLoS Genet. *10*, e1004394.

Douglas, S.J., Dawson-Scully, K., and Sokolowski, M.B. (2005). The neurogenetics and evolution of food-related behaviour. Trends Neurosci. *28*, 644–652.

Erhardt, S., Blennow, K., Nordin, C., Skogh, E., Lindström, L.H., and Engberg, G. (2001). Kynurenic acid levels are elevated in the cerebrospinal fluid of patients with schizophrenia. Neurosci. Lett. *313*, 96–98.

Erhardt, S., Lim, C.K., Linderholm, K.R., Janelidze, S., Lindqvist, D., Samuelsson, M., Lundberg, K., Postolache, T.T., Träskman-Bendz, L., Guillemin, G.J., and Brundin, L. (2013). Connecting inflammation with glutamate agonism in suicidality. Neuropsychopharmacology *38*, 743–752.

Foster, A.C., Vezzani, A., French, E.D., and Schwarcz, R. (1984). Kynurenic acid blocks neurotoxicity and seizures induced in rats by the related brain metabolite quinolinic acid. Neurosci. Lett. *48*, 273–278.

Gray, J.M., Hill, J.J., and Bargmann, C.I. (2005). A circuit for navigation in Caenorhabditis elegans. Proc. Natl. Acad. Sci. USA *102*, 3184–3191.

Greer, E.R., Pérez, C.L., Van Gilst, M.R., Lee, B.H., and Ashrafi, K. (2008). Neural and molecular dissection of a C. elegans sensory circuit that regulates fat and feeding. Cell Metab. *8*, 118–131.

Heyes, M.P., Saito, K., Crowley, J.S., Davis, L.E., Demitrack, M.A., Der, M., Dilling, L.A., Elia, J., Kruesi, M.J.P., Lackner, A., et al. (1992). Quinolinic acid and kynurenine pathway metabolism in inflammatory and non-inflammatory neurological disease. Brain *115*, 1249–1273.

Hills, T., Brockie, P.J., and Maricq, A.V. (2004). Dopamine and glutamate control area-restricted search behavior in Caenorhabditis elegans. J. Neurosci. *24*, 1217–1225.

Hilmas, C., Pereira, E.F.R., Alkondon, M., Rassoulpour, A., Schwarcz, R., and Albuquerque, E.X. (2001). The brain metabolite kynurenic acid inhibits α7 nicotinic receptor activity and increases non-α7 nicotinic receptor expression: physiopathological implications. J. Neurosci. *21*, 7463–7473.

Horvitz, H.R., Chalfie, M., Trent, C., Sulston, J.E., and Evans, P.D. (1982). Serotonin and octopamine in the nematode Caenorhabditis elegans. Science *216*, 1012–1014.

Kao, G., Nordenson, C., Still, M., Rönnlund, A., Tuck, S., and Naredi, P. (2007). ASNA-1 positively regulates insulin secretion in C. elegans and mammalian cells. Cell *128*, 577–587.

Kubiak, T.M., Larsen, M.J., Bowman, J.W., Geary, T.G., and Lowery, D.E. (2008). FMRFamide-like peptides encoded on the flp-18 precursor gene activate two isoforms of the orphan Caenorhabditis elegans G-protein-coupled receptor Y58G8A.4 heterologously expressed in mammalian cells. Biopolymers *90*, 339–348.

Lam, T.K.T. (2010). Neuronal regulation of homeostasis by nutrient sensing. Nat. Med. *16*, 392–395.

Lapin, I.P., and Oxenkrug, G.F. (1969). Intensification of the central serotoninergic processes as a possible determinant of the thymoleptic effect. Lancet *1*, 132–136.

Lee, B.H., Liu, J., Wong, D., Srinivasan, S., and Ashrafi, K. (2011). Hyperactive neuroendocrine secretion causes size, feeding, and metabolic defects of C. elegans Bardet-Biedl syndrome mutants. PLoS Biol. *9*, e1001219.

Li, W., Kennedy, S.G., and Ruvkun, G. (2003). daf-28 encodes a C. elegans insulin superfamily member that is regulated by environmental cues and acts in the DAF-2 signaling pathway. Genes Dev. *17*, 844–858.

Liang, B., Moussaif, M., Kuan, C.-J., Gargus, J.J., and Sze, J.Y. (2006). Serotonin targets the DAF-16/FOXO signaling pathway to modulate stress responses. Cell Metab. *4*, 429–440.

Liu, T., Kong, D., Shah, B.P., Ye, C., Koda, S., Saunders, A., Ding, J.B., Yang, Z., Sabatini, B.L., and Lowell, B.B. (2012). Fasting activation of AgRP neurons requires NMDA receptors and involves spinogenesis and increased excitatory tone. Neuron *73*, 511–522.

McElroy, S.L., and Keck, P.E., Jr. (2014). Metabolic syndrome in bipolar disorder: a review with a focus on bipolar depression. J. Clin. Psychiatry *75*, 46–61.

Mitchell, A.J., Vancampfort, D., Sweers, K., van Winkel, R., Yu, W., and De Hert, M. (2013). Prevalence of metabolic syndrome and metabolic abnormalities in schizophrenia and related disorders—a systematic review and meta-analysis. Schizophr. Bull. *39*, 306–318.

Perkins, M.N., and Stone, T.W. (1982). An iontophoretic investigation of the actions of convulsant kynurenines and their interaction with the endogenous excitant quinolinic acid. Brain Res. *247*, 184–187.

Piggott, B.J., Liu, J., Feng, Z., Wescott, S.A., and Xu, X.Z.S. (2011). The neural circuits and synaptic mechanisms underlying motor initiation in C. elegans. Cell *147*, 922–933.

Sawin, E.R., Ranganathan, R., and Horvitz, H.R. (2000). C. elegans locomotory rate is modulated by the environment through a dopaminergic pathway and by experience through a serotonergic pathway. Neuron *26*, 619–631.

Schwarcz, R., Rassoulpour, A., Wu, H.-Q., Medoff, D., Tamminga, C.A., and Roberts, R.C. (2001). Increased cortical kynurenate content in schizophrenia. Biol. Psychiatry *50*, 521–530.

Schwarcz, R., Bruno, J.P., Muchowski, P.J., and Wu, H.-Q. (2012). Kynurenines in the mammalian brain: when physiology meets pathology. Nat. Rev. Neurosci. *13*, 465–477.

Sengupta, P. (2013). The belly rules the nose: feeding state-dependent modulation of peripheral chemosensory responses. Curr. Opin. Neurobiol. *23*, 68–75.

Song, B.M., Faumont, S., Lockery, S., and Avery, L. (2013). Recognition of familiar food activates feeding via an endocrine serotonin signal in Caenorhabditis elegans. eLife *2*, e00329.

Srinivasan, S., Sadegh, L., Elle, I.C., Christensen, A.G.L., Faergeman, N.J., and Ashrafi, K. (2008). Serotonin regulates C. elegans fat and feeding through independent molecular mechanisms. Cell Metab. *7*, 533–544.

Steiner, J., Walter, M., Gos, T., Guillemin, G.J., Bernstein, H.-G., Sarnyai, Z., Mawrin, C., Brisch, R., Bielau, H., Meyer zu Schwabedissen, L., et al. (2011). Severe depression is associated with increased microglial quinolinic acid in subregions of the anterior cingulate gyrus: evidence for an immune-modulated glutamatergic neurotransmission? J. Neuroinflammation *8*, 94.

Stipanuk, M.H., and Caudill, M.A. (2013). Biochemical, Physiological, and Molecular Aspects of Human Nutrition (Philadelphia, PA: Elsevier Health Sciences).

Sze, J.Y., Victor, M., Loer, C., Shi, Y., and Ruvkun, G. (2000). Food and metabolic signalling defects in a Caenorhabditis elegans serotonin-synthesis mutant. Nature *403*, 560–564.

Taylor, R.C., Berendzen, K.M., and Dillin, A. (2014). Systemic stress signalling: understanding the cell non-autonomous control of proteostasis. Nat. Rev. Mol. Cell Biol. *15*, 211–217.

Tian, L., Hires, S.A., Mao, T., Huber, D., Chiappe, M.E., Chalasani, S.H., Petreanu, L., Akerboom, J., McKinney, S.A., Schreiter, E.R., et al. (2009). Imaging neural activity in worms, flies and mice with improved GCaMP calcium indicators. Nat. Methods *6*, 875–881.

van der Goot, A.T., and Nollen, E.A.A. (2013). Tryptophan metabolism: entering the field of aging and age-related pathologies. Trends Mol. Med. *19*, 336–344.

van der Goot, A.T., Zhu, W., Vázquez-Manrique, R.P., Seinstra, R.I., Dettmer, K., Michels, H., Farina, F., Krijnen, J., Melki, R., Buijsman, R.C., et al. (2012). Delaying aging and the aging-associated decline in protein homeostasis by inhibition of tryptophan degradation. Proc. Natl. Acad. Sci. USA *109*, 14912–14917.

Waggoner, L.E., Hardaker, L.A., Golik, S., and Schafer, W.R. (2000). Effect of a neuropeptide gene on behavioral states in Caenorhabditis elegans egg-laying. Genetics *154*, 1181–1192.

Whim, M.D., and Moss, G.W.J. (2001). A novel technique that measures peptide secretion on a millisecond timescale reveals rapid changes in release. Neuron *30*, 37–50.

White, J.G., Southgate, E., Thomson, J.N., and Brenner, S. (1986). The structure of the nervous system of the nematode Caenorhabditis elegans. Philos. Trans. R. Soc. Lond. B Biol. Sci. *314*, 1–340.

You, Y.J., Kim, J., Raizen, D.M., and Avery, L. (2008). Insulin, cGMP, and TGF-β signals regulate food intake and quiescence in C. elegans: a model for satiety. Cell Metab. *7*, 249–257.

Zwilling, D., Huang, S.-Y., Sathyasaikumar, K.V., Notarangelo, F.M., Guidetti, P., Wu, H.-Q., Lee, J., Truong, J., Andrews-Zwilling, Y., Hsieh, E.W., et al. (2011). Kynurenine 3-monooxygenase inhibition in blood ameliorates neurodegeneration. Cell *145*, 863–874.